

Supporting information

Facile Synthesis of Highly Stable and Well-Dispersed Mesoporous ZrO₂/FDU-15 Composites with High Performance in Oxidative Dehydrogenation of Ethylbenzene

Qiang Li, Jie Xu, Zhangxiong Wu, Dan Feng, Jianping Yang, Jing Wei, Qingling Wu, Bo Tu, Yong Cao and Dongyuan Zhao*

Department of Chemistry and Shanghai Key Laboratory of Molecular Catalysis and Innovative Materials, Laboratory of Advanced Materials, Fudan University, Shanghai 200433, People's Republic of China

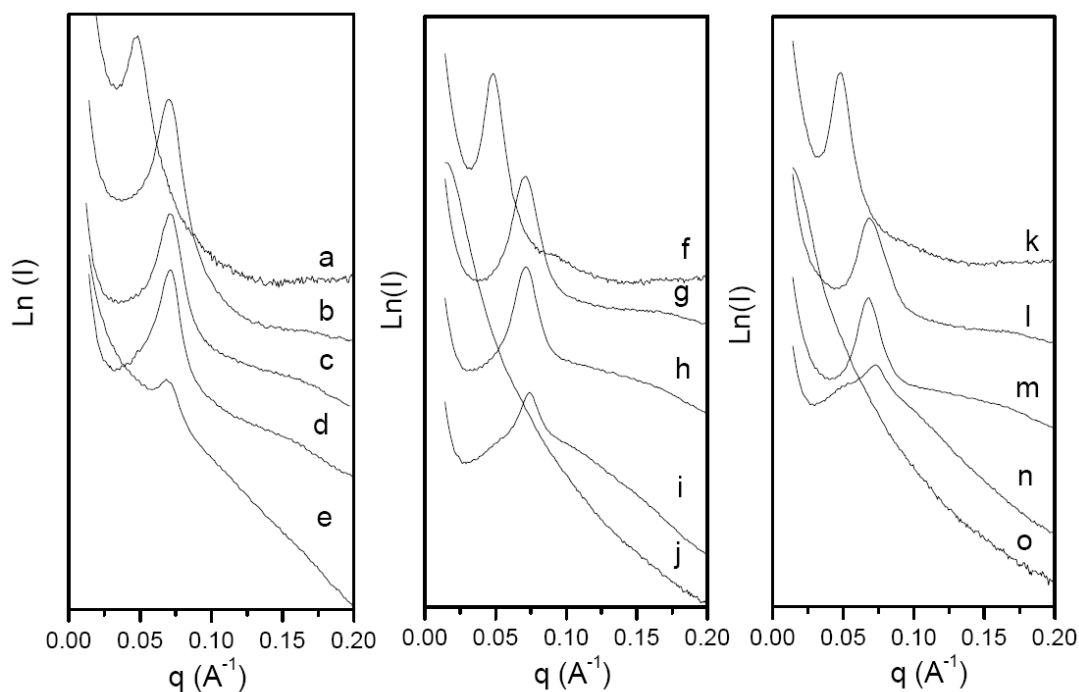


Fig. S1 SAXS patterns of mesoporous zirconia/FDU-15 composites with different zirconium contents and pyrolysis temperatures: (a) ZC-II-as-made; (b) ZC-II-600; (c) ZC-II-700; (d) ZC-II-800; (e) ZC-II-900; (f) ZC-III-as-made; (g) ZC-III-600; and (h) ZC-III-700; (i) ZC-III-800; (j) ZC-III-900; (k) ZC-IV-as-made; (l) ZC-IV-600; (m) ZC-IV-700; (n) ZC-IV-800; (o) ZC-IV-900.

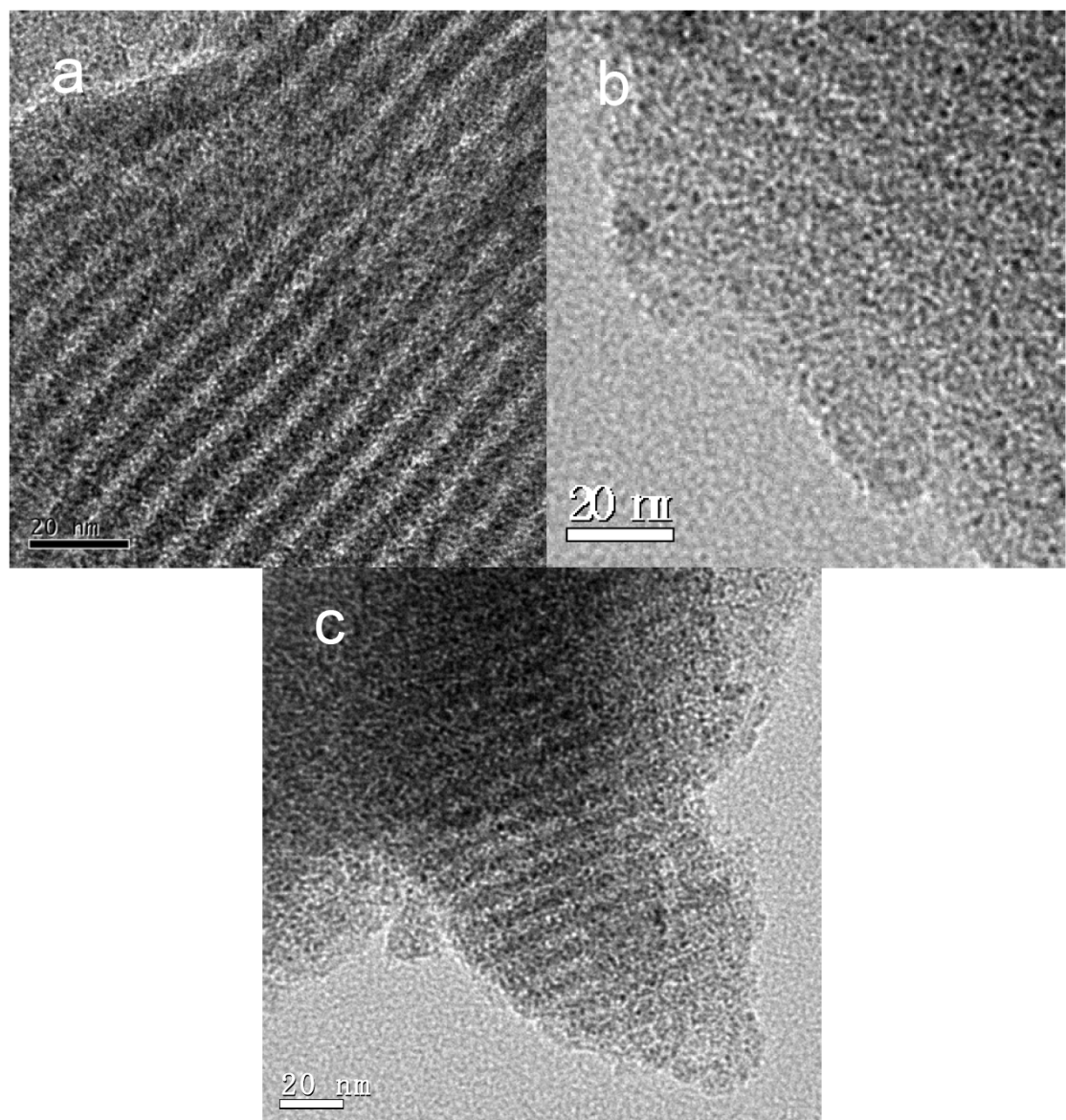


Fig. S2 TEM images of mesoporous $\text{ZrO}_2/\text{FDU}-15$ composites: (a) ZC-II -600; (b) ZC-III -600; (c) ZC-IV-600.

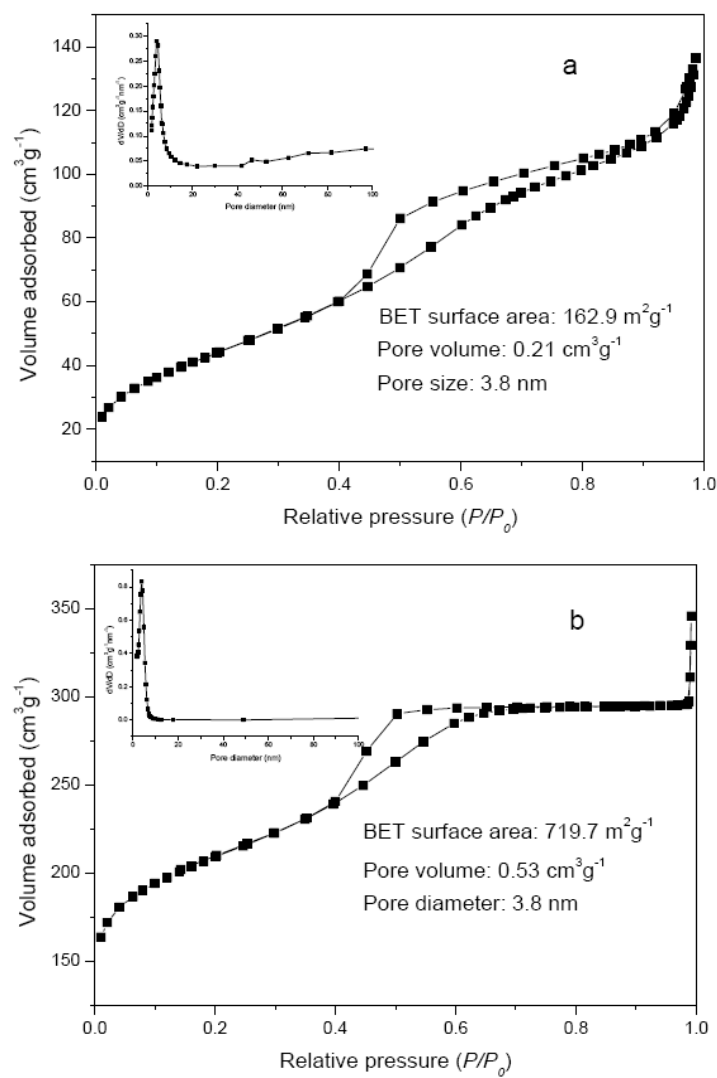


Fig. S3 Nitrogen sorption isotherms and corresponding pore size distributions of (a) mesoporous zirconia (Meso-ZrO₂) and (b) pristine mesoporous carbon FDU-15.

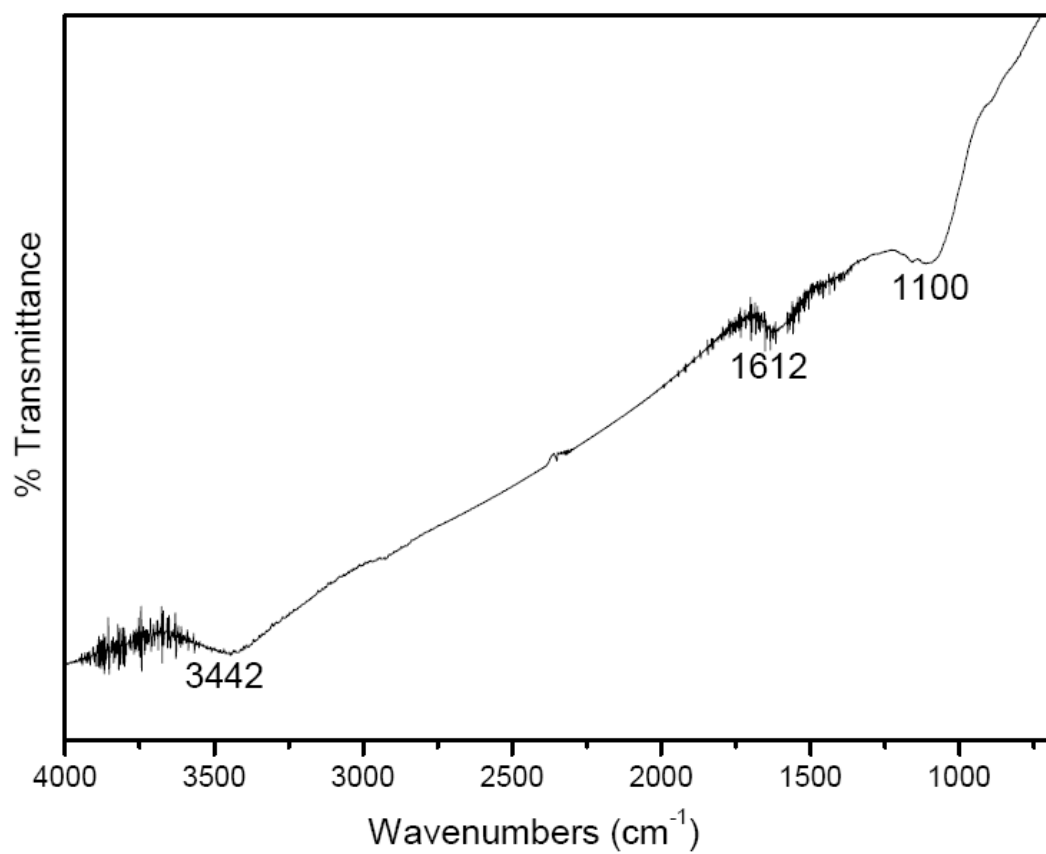


Fig. S4 FT-IR spectrum of pristine mesoporous carbon FDU-15.

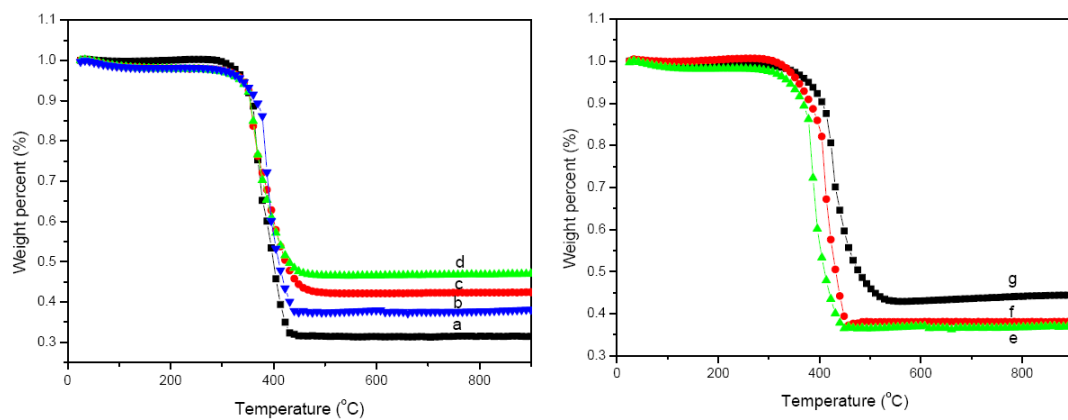


Fig. S5 TG curves of mesoporous $\text{ZrO}_2/\text{FDU-15}$ composites under air atmosphere. (a) ZC-I-600; (b) ZC-II-600; (c) ZC-III-600; (d) ZC-IV-600; (e) ZC-I-700; (f) ZC-I-800; and (g) ZC-I-900.